



## SIMPLE INTEGRAL FUZZY CONTROL FOR CONVERTERS WITH HIGHLY NONLINEAR DYNAMICS

Kuang-Yow Lian

*Department of Electrical Engineering, National Taipei University of Technology, Taipei, Taiwan, R.O.C.,  
ylian@ntut.edu.tw*

Chi-Wang Hong

*Department of Electrical Engineering, Chung-Yuan Christian University, Chung-Li, Taiwan, R.O.C.*

Follow this and additional works at: <https://jmstt.ntou.edu.tw/journal>



Part of the [Electrical and Computer Engineering Commons](#)

### Recommended Citation

Lian, Kuang-Yow and Hong, Chi-Wang (2014) "SIMPLE INTEGRAL FUZZY CONTROL FOR CONVERTERS WITH HIGHLY NONLINEAR DYNAMICS," *Journal of Marine Science and Technology*. Vol. 22: Iss. 5, Article 4.

DOI: 10.6119/JMST-013-0710-1

Available at: <https://jmstt.ntou.edu.tw/journal/vol22/iss5/4>

This Research Article is brought to you for free and open access by Journal of Marine Science and Technology. It has been accepted for inclusion in Journal of Marine Science and Technology by an authorized editor of Journal of Marine Science and Technology.

# SIMPLE INTEGRAL FUZZY CONTROL FOR CONVERTERS WITH HIGHLY NONLINEAR DYNAMICS

Kuang-Yow Lian<sup>1</sup> and Chi-Wang Hong<sup>2</sup>

Key words: T-S fuzzy model, nonlinear integral control, linear matrix inequalities (LMIs), power factor correction (PFC).

## ABSTRACT

A simple integral Takagi-Sugeno (T-S) fuzzy control scheme suitable for many types of converters is proposed in this paper. A converter with highly nonlinear characteristics, called active high power factor correction (AHPFC), is taken as an example to show the control scheme. Indeed, we can derive a linear controller to achieve zero output regulation error for the AHPFC converter. First, we include an integral error signal to form an augmented system. After translating the coordinate to the regulated point, we obtain the stabilization model. The model-based fuzzy approach is then used to handle the nonlinear system. The system stability is proven by Lyapunov theorem. The feedback gains are obtained by solving linear matrix inequalities (LMIs). A surprised property is that the gains are identical for every fuzzy control rule. This result greatly simplifies the controller to be a linear state feedback one. Finally, the simulation and experimental results show the satisfactory performance, which is better than the converter using a proportional integral (PI) controller.

## I. INTRODUCTION

In recent years, the electronic technologies have rapidly been expanded worldwide. As the power sources of computers, consumer devices and communication equipment (i.e., 3C electronic products), the power supplies are required with high performance, reliability and stability. Instead of the linear power supplies, the switching converters are promising due to their high efficiencies. However, the converters possess inherently nonlinear characteristics. Particularly, AC-DC iso-

lated converters [16, 20, 28] take the power factor correction (PFC) into consideration and thus have heavy nonlinear properties when compared to the basic DC-DC converters, e.g., buck, boost, buck-boost, forward and flyback converters, etc. They are often too complex to be analyzed and controlled, since a switching period has several time-subinterval stages. Generally, PFC converters need two controllers to achieve two purposes, the power factor correction and the output voltage regulation [16]. As a demonstration of designing controller, an active-high-power-factor-correction (AHPFC) converter is considered here, which accomplishes two aforementioned purposes in discontinuous conduction mode (DCM) using one controller by the classical linear methods in [14]. In this paper, we will derive a simple feedback controller for the AHPFC converter via a nonlinear design approach.

In the past years, many approaches were proposed for the pulse-width-modulation (PWM) switching control design, e.g., proportional integral (PI) control, sliding mode control, Mamdani-type fuzzy control, fuzzy neural control, and  $H_\infty$  control, etc. [6, 7, 10, 17, 22]. There are some shortcomings in these strategies. For example, it is complicated to determine the transfer functions from duty ratios to output voltages using the linear control techniques, which are difficult to govern the internal nonlinear states of the converters, e.g., inductor current and capacitor voltage [15, 27]. On the other hand, the stability of the system using model-free fuzzy methods cannot be analyzed by theoretical method, and its fuzzy sets are chosen by trial-and-error procedures or by experience [8, 18, 19, 25, 26]. Therefore, the question of "how to design an intelligent controller for the switching power converters instead of a conventional one" has been attracting a lot of attention recently.

Compared to the traditional fuzzy methods, the stability of Takagi-Sugeno (T-S) fuzzy scheme [21] can be rigorously proven by Lyapunov theorem. Significantly, the linear matrix inequality (LMI) can powerfully reduce the issues of the stability analysis and the control design for a T-S fuzzy modeling system with a parallel distributed compensation (PDC) structure [1, 23, 24]. Consequently, model-based fuzzy control and LMIs method are combined together to cope with the different nonlinear problems, e.g., ship steering systems, truck-trailer

Paper submitted 05/30/12; revised 04/29/13; accepted 07/10/13. Author for correspondence: Kuang-Yow Lian (e-mail: kylian@ntut.edu.tw).

<sup>1</sup>Department of Electrical Engineering, National Taipei University of Technology, Taipei, Taiwan, R.O.C.

<sup>2</sup>Department of Electrical Engineering, Chung-Yuan Christian University, Chung-Li, Taiwan, R.O.C.

system and drum-boiler system, etc. [2-5, 9]. Furthermore, the integral control can effectively achieve zero steady-state error for the constant exogenous disturbances. The advantages of integral fuzzy control approach for switching power converters are to dealing with the nonlinear dynamics and the constant bias to achieve the perfect output voltage regulation. Hence, the LMI-based integral T-S fuzzy model is proposed to control DC-DC converters and permanent-magnet synchronous motors [11-13]. Here, we attempt to apply the integral T-S fuzzy control scheme to the AHPFC converter, where the design challenge comes from how to obtain simple controller from complex equations.

Comparing with the previous research [11], the motivation of this paper is generally to construct a uniform controller, which is suitable for many types of converters. For simplifying the integral T-S fuzzy controller, we systematically describe the design procedure and the implementation steps via a unified LMI approach. First, we derive the dynamics of the AHPFC converter by using the average methods of two-time-scale discontinuous system (AM-TTS-DS). Next, we offer the integral T-S fuzzy model to the converters with an emphasis on dealing with the nonlinear characters. The exponential stability is proven by Lyapunov method whereas the control gains are obtained via Matlab toolbox. A special property is that the obtained gains are identical for every fuzzy control rule, i.e.,  $K_{11} = K_{21} = K_{31} = K_{41}$ , etc. Therefore, the control law can be simplified further as a linear feedback controller, which can be easily implemented by using simple analog circuits. Finally, the performance is successfully confirmed by the numerical simulations and hardware experiments. It is noteworthy that the challenges for the Mamdani-type controller and the general T-S fuzzy controller are the implementation of the membership functions and the fuzzy rules. Instead of using DSP or FPGA, the proposed integral T-S fuzzy controller has been implemented using analog circuits to achieve satisfactory performance without steady-state error.

## II. DYNAMIC ANALYSIS FOR AHPFC CONVERTERS

This section introduces the operation principle of an AHPFC converter and derives its dynamical equation to represent the switching property. The practical circuit of the converter is illustrated in Fig. 1, which is combined by a PFC cell with a regulator. Here,  $M$  denotes the power switch MOSFET;  $R$  is the output load resistance;  $D_1$ ,  $D_2$  and  $D_3$  are the diodes;  $L$  is the inductor;  $L_m$  is the exciting inductor;  $V_g$  is the rectified input voltage.  $V_p$  and  $V_s$  are the primary and the secondary voltages of the transformer with turns ratio  $n$ ;  $V_{C_p}$  and  $V_{C_s}$  are the voltages of the capacitors  $C_p$  and  $C_s$ , respectively. The converter is operated in a steady-state condition and the bulk capacitor  $C_p$  is large enough for a constant voltage across it. One switching period  $T_s$  can be divided into four time subinterval stages: Stage 1, duty ratio  $d_1$  ( $M$ : on,  $D_1$ : on,  $D_2$ : off,  $D_3$ : off); Stage 2,  $d_2$  ( $M$ : off,  $D_1$ : off,  $D_2$ : on,  $D_3$ : on); Stage 3,

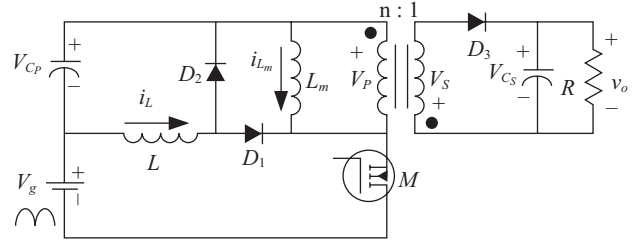


Fig. 1. An AHPFC converter.

$d_3$  ( $M$ : off,  $D_1$ : off,  $D_2$ : off,  $D_3$ : on); and Stage 4,  $d_4$  ( $M$ : off,  $D_1$ : off,  $D_2$ : off,  $D_3$ : off).

To achieve high power factor corrections,  $L$  and  $L_m$  are operated in discontinuous conduction mode (DCM). It implies  $i_L(0) = i_L(T_s) = 0$  and  $i_{L_m}(0) = i_{L_m}(T_s) = 0$ . We can obtain the following states:

$$\begin{aligned} C_p \langle \dot{v}_{C_p}(t) \rangle_{T_s} &= \langle i_{C_p}(t) \rangle_{T_s} \\ C_s \langle \dot{v}_{C_s}(t) \rangle_{T_s} &= \langle i_{C_s}(t) \rangle_{T_s}, \end{aligned} \tag{1}$$

where  $\langle \bullet \rangle_{T_s}$  is the average function during a switching period.

Hence, the storage components are denoted as

$$\begin{aligned} \langle v_L \rangle_{T_s} &= \frac{1}{T_s} \left( d_1 T_s \langle V_g \rangle_{T_s} - d_2 T_s \langle v_{C_p} \rangle_{T_s} \right), \\ \langle v_{L_m} \rangle_{T_s} &= \frac{1}{T_s} \left( d_1 T_s \left( \langle V_g \rangle_{T_s} + \langle v_{C_p} \rangle_{T_s} \right) - n(d_2 + d_3) T_s \langle v_{C_s} \rangle_{T_s} \right), \\ \langle i_{C_p} \rangle_{T_s} &= \frac{1}{T_s} \left( d_1^2 T_s \frac{\langle V_g \rangle_{T_s} + \langle v_{C_p} \rangle_{T_s}}{2L_m} + (d_2 T_s)^2 \frac{\langle v_{C_p} \rangle_{T_s}}{2L} \right), \\ \langle i_{C_s} \rangle_{T_s} &= \frac{1}{T_s} \left( -(d_1 + d_2 + d_3 + d_4) T_s \frac{\langle v_{C_s} \rangle_{T_s}}{R} \right. \\ &\quad \left. + (d_2 + d_3)^2 T_s \frac{n^2 \langle v_{C_s} \rangle_{T_s}}{2L_m} \right). \end{aligned}$$

According to the voltage-second balance law, the average voltage of the inductors,  $\langle v_L \rangle_{T_s}$  and  $\langle v_{L_m} \rangle_{T_s}$ , are equal to zero, respectively. The relationships of the duty ratio  $d_1$  with  $d_2$ ,  $d_3$ , and  $d_4$  can be found as

$$d_2 = \frac{\langle V_g \rangle_{T_s}}{\langle v_{C_p} \rangle_{T_s}} d_1,$$

$$d_3 = \left( \frac{\langle V_g \rangle_{T_s} + \langle v_{C_p} \rangle_{T_s}}{n \langle v_{C_s} \rangle_{T_s}} - \frac{\langle V_g \rangle_{T_s}}{\langle v_{C_p} \rangle_{T_s}} \right) d_1,$$

$$d_4 = 1 - d_1 - d_2 - d_3 = 1 - \left( 1 + \frac{\langle V_g \rangle_{T_s} + \langle v_{C_p} \rangle_{T_s}}{n \langle v_{C_s} \rangle_{T_s}} \right) d_1.$$

The states are expressed as follows:

$$C_p \langle \dot{v}_{C_p} \rangle_{T_s} = d_1^2 \frac{\langle V_g \rangle_{T_s} + \langle v_{C_p} \rangle_{T_s}}{2L_m} + (d_2^2 T_s) \frac{\langle v_{C_p} \rangle_{T_s}}{2L}$$

$$C_s \langle \dot{v}_{C_s} \rangle_{T_s} = -(d_1 + d_2 + d_3 + d_4) \frac{\langle v_{C_p} \rangle_{T_s}}{R}$$

$$+ (d_2 + d_3)^2 \frac{n^2 \langle v_{C_s} \rangle_{T_s}}{2L_m}, \quad (2)$$

Due to the switching frequency 100 kHz is faster than the haversine frequency 120 Hz,  $V_g$  can be assumed as a constant value, i.e.,  $\langle V_g \rangle_{T_s} = V_g$ , during the switching period. Furthermore, we substitute  $d_2$ ,  $d_3$ , and  $d_4$  into (2) and consider  $V_g = |V_m \sin(\omega t)|$  during a haversine period  $T_L$ . After combining the affections of the faster variable on the slower variable, the average dynamics via AM-TTS-DS method is derived as follows:

$$\dot{\mathbf{v}}_{C_p} = \frac{d_1^2(t) T_s}{2C_p} \left( \frac{V_m^2}{2L \mathbf{v}_{C_p}} - \frac{2V_m}{\pi L_m} - \frac{\mathbf{v}_{C_p}}{L_m} \right)$$

$$\dot{\mathbf{v}}_{C_s} = \frac{d_1^2(t) T_s}{2L_m C_s \mathbf{v}_{C_s}} \left( \frac{V_m^2}{2} + \frac{4V_m \mathbf{v}_{C_p}}{\pi} + \mathbf{v}_{C_p}^2 \right) - \frac{\mathbf{v}_{C_s}}{RC_s}, \quad (3)$$

where  $\mathbf{v}_{C_p} = \langle \langle v_{C_p} \rangle_{T_s} \rangle_{T_L}$ ,  $\mathbf{v}_{C_s} = \langle \langle v_{C_s} \rangle_{T_s} \rangle_{T_L}$  and  $d_1$  is a control input. The system (3) is nonlinear since the control input is two state-dependents, e.g.,  $d_1^2(t)$  is multiplied by  $\mathbf{v}_{C_p}(t)$  and divided by  $\mathbf{v}_{C_s}(t)$ , etc.

### III. INTEGRAL T-S FUZZY REGULATOR

In this section, we propose an integral Takagi-Sugeno (T-S) fuzzy control scheme to deal with the aforementioned nonlinear system. The sequences of control design are described as the following five steps.

#### 1. Integral-type Control Strategy

Consider a general nonlinear system for the dynamic model (3) as follows:

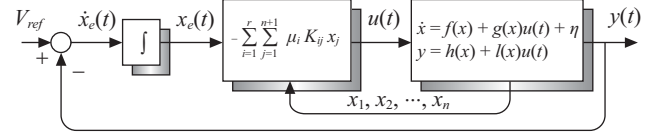


Fig. 2. Sketched diagram of the integral T-S fuzzy control.

$$\dot{x}_p(t) = f(x_p(t)) + g(x_p(t))u(t) + \eta$$

$$y(t) = h(x_p(t)) + l(x_p(t))u(t), \quad (4)$$

where  $x_p(t) \in R^n$ ,  $u(t) \in R^m$ ,  $y(t) \in R^m$  are the state, the control input, and the output vectors, respectively; and  $\eta$  is the constant bias term. The conceptual diagram of the integral T-S fuzzy control is depicted in Fig. 2. Here, the control input  $u(t)$  represents the duty cycle  $d_1(t)$ ;  $V_{ref}$  is the constant reference; and  $y(t)$  denotes the output voltage  $\mathbf{v}_{C_s}(t)$  for the AHPFC converter. Then, we want to design the integral T-S fuzzy controller such that  $y(t) \rightarrow V_{ref}$  as  $t \rightarrow \infty$ .

To achieve zero steady-state error, we use the integral-type method to design a sturdy controller that can minimize uncertainties and exogenous disturbances. A new state variable,  $x_e(t) = \int (V_{ref} - y(t))dt$ , is accounted for the integral of the output regulation error, which results in the error dynamic,  $\dot{x}_e(t) = V_{ref} - y(t)$ . Therefore, the augmented dynamics of the model (3) are formed as follows:

$$\dot{x}_1 = \frac{d_1^2(t) T_s}{2L_m C_s x_1} \left( \frac{V_m^2}{2} + \frac{4V_m x_2}{\pi} + x_2^2 \right) - \frac{x_1}{RC_s}$$

$$\dot{x}_2 = \frac{d_1^2(t) T_s}{2C_p} \left( \frac{V_m^2}{2L x_2} - \frac{2V_m}{\pi L_m} - \frac{x_2}{L_m} \right)$$

$$\dot{x}_3 = V_{ref} - x_1, \quad (5)$$

where  $x_1 = \mathbf{v}_{C_s}$ ,  $x_2 = \mathbf{v}_{C_p}$ , and  $x_3 = x_e$ . Then, we will derive the stabilization model of the converter via translating coordinates.

#### 2. Coordinate Translation to Operation Points

The objective of the output regulation is realized by stabilizing the system at an equilibrium state, which produces  $\mathbf{v}_{C_s}(t) = V_{ref}$ . Firstly, we need to find  $\bar{x}_p$  and  $\bar{u}$  that are the equilibrium points of the state  $x_p(t)$  and the control input  $u(t)$ , respectively. For this purpose, let the right-hand side of (5) to be zero, we can obtain the equilibrium points as follows:

$$\bar{x}_1 = V_{ref}$$

$$\bar{x}_2 = \left( \sqrt{\frac{1}{\pi^2} + \frac{L_m}{2L}} - \frac{1}{\pi} \right) V_m$$

$$\bar{d}_1 = \frac{V_{ref}}{\left( \sqrt{\frac{RT_s}{2L_m} \left( \frac{1}{2} \left( 1 + \frac{L_m}{L} \right) + \frac{2}{\pi} \left( \sqrt{\frac{1}{\pi^2} + \frac{L_m}{2L} - \frac{1}{\pi}} \right) \right)} \right)} V_m \quad (6)$$

Secondly, let  $x_1(t) = \tilde{x}_1(t) + \bar{x}_1$ ,  $x_2(t) = \tilde{x}_2(t) + \bar{x}_2$ ,  $x_3(t) = \tilde{x}_3(t) + \bar{x}_3$ , and  $d_1(t) = \tilde{d}_1(t) + \bar{d}_1$ . As a designed parameter for the integral control, the equilibrium point  $\bar{x}_3 = \bar{x}_e$  will be determined later. After substituting (6) into (5), we obtain the following model:

$$\begin{aligned} \dot{\tilde{x}}_1 &= \frac{1}{C_s} \left( \frac{(\tilde{d}_1 + \bar{d}_1)^2 T_s}{2L_m (\tilde{x}_1 + \bar{x}_1)} \left( \frac{V_m^2}{2} + \frac{4V_m x_2}{\pi} + (\tilde{x}_2 + \bar{x}_2)^2 \right) - \frac{\tilde{x}_1}{R} \right) \\ \dot{\tilde{x}}_2 &= \frac{1}{C_p} \left( \frac{(\tilde{d}_1 + \bar{d}_1)^2 T_s}{2} \right) \left( \frac{V_m^2}{2L(\tilde{x}_2 + \bar{x}_2)} - \frac{2V_m}{\pi L_m} - \frac{\tilde{x}_2}{L_m} \right) \\ \dot{\tilde{x}}_3 &= V_{ref} - (\tilde{x}_1 + \bar{x}_1). \end{aligned}$$

After excluding the higher-order terms by substituting them with relatively small values, we can rewrite the model as follows:

$$\begin{aligned} \begin{bmatrix} \dot{\tilde{x}}_1 \\ \dot{\tilde{x}}_2 \\ \dot{\tilde{x}}_3 \end{bmatrix} &= \begin{bmatrix} \Psi & \frac{\bar{d}_1^2 T_s}{2L_m C_s \bar{x}_1} (4V_m + 2\pi \bar{x}_2) & 0 \\ 0 & -\frac{\bar{d}_1^2 T_s}{2C_p} \left( \frac{1}{L_m} + \frac{V_m^2}{2L\bar{x}_2^2} \right) & 0 \\ -1 & 0 & 0 \end{bmatrix} \begin{bmatrix} \tilde{x}_1 \\ \tilde{x}_2 \\ \tilde{x}_3 \end{bmatrix} \\ &+ \begin{bmatrix} \frac{\bar{d}_1 T_s}{\pi L_m C_s \bar{x}_1} \Theta - \frac{\bar{d}_1 T_s}{\pi L_m C_s \bar{x}_1^2} \theta \tilde{x}_1 \\ \frac{\bar{d}_1 T_s}{C_p} \left( \frac{V_m^2}{2L\bar{x}_2} - \frac{2V_m}{\pi L_m} - \frac{\bar{x}_2}{L_m} - \left( \frac{1}{L_m} + \frac{V_m^2}{2L\bar{x}_2^2} \right) \tilde{x}_2 \right) \\ 0 \end{bmatrix} \tilde{d}_1 \quad (7) \end{aligned}$$

where  $\Psi = -\frac{1}{C_s} \left( \frac{1}{R} + \frac{\bar{d}_1^2 T_s}{2\pi L_m \bar{x}_1^2} \Theta \right)$ ,  $\Theta = \theta + (4V_m + 2\pi \bar{x}_2)$  and  $\theta = 0.5\pi V_m^2 + 4V_m \bar{x}_2 + \pi \bar{x}_2^2$ . Then, we need to deal with the nonlinear characteristics of the converter.

### 3. Establishment of Integral T-S Fuzzy Modeling System

According to the modeling approach, the dynamic system (7) with nonlinear terms can be accurately represented by the integral T-S fuzzy model as the following rules:

**Plant Rule  $i$ :**

IF  $\tilde{x}_1(t)$  is  $F_{1i}$  and  $\tilde{x}_2(t)$  is  $F_{2i}$  THEN  
 $\dot{\tilde{x}}(t) = A_i \tilde{x}(t) + B_i \tilde{u}(t)$ ,  $i = 1, 2, 3, 4$ ,

where  $\tilde{x}(t) = [\tilde{x}_1(t) \ \tilde{x}_2(t) \ \tilde{x}_3(t)]^T$ ;  $F_{1i}$  and  $F_{2i}$  ( $i = 1, 2, 3, 4$ ) are fuzzy sets. Moreover, let

$$\phi_1 = 0.5\pi V_m^2 + 4V_m \bar{x}_2 + \pi \bar{x}_2^2 + (4V_m + 2\pi \bar{x}_2)\beta,$$

$$\Phi_1 = \frac{1}{R} + \frac{\bar{d}_1^2 T_s}{2\pi L_m \bar{x}_1^2} \phi_1,$$

$$\phi_2 = 0.5\pi V_m^2 + 4V_m \bar{x}_2 + \pi \bar{x}_2^2 - (4V_m + 2\pi \bar{x}_2)\beta,$$

$$\Phi_2 = \frac{1}{R} + \frac{\bar{d}_1^2 T_s}{2\pi L_m \bar{x}_1^2} \phi_2.$$

Here,  $\alpha$  and  $\beta$  denote the intervals that  $\tilde{x}_1$  and  $\tilde{x}_2$  lies within, i.e.,  $\tilde{x}_1 \in \{-\alpha, \alpha\}$  and  $\tilde{x}_2 \in \{-\beta, \beta\}$ . We can obtain the subsystem matrices as follows:

$$\begin{aligned} A_1 = A_2 &= \begin{bmatrix} -\frac{1}{C_s} \Phi_1 & \frac{\bar{d}_1^2 T_s}{2L_m C_s \bar{x}_1} (4V_m + 2\pi \bar{x}_2) & 0 \\ 0 & -\frac{\bar{d}_1^2 T_s}{2C_p} \left( \frac{1}{L_m} + \frac{V_m^2}{2L\bar{x}_2^2} \right) & 0 \\ -1 & 0 & 0 \end{bmatrix}, \\ A_3 = A_4 &= \begin{bmatrix} -\frac{1}{C_s} \Phi_2 & \frac{\bar{d}_1^2 T_s}{2L_m C_s \bar{x}_1} (4V_m + 2\pi \bar{x}_2) & 0 \\ 0 & -\frac{\bar{d}_1^2 T_s}{2C_p} \left( \frac{1}{L_m} + \frac{V_m^2}{2L\bar{x}_2^2} \right) & 0 \\ -1 & 0 & 0 \end{bmatrix}, \\ B_i &= \begin{bmatrix} \frac{\bar{d}_1 T_s}{\pi L_m C_s L \bar{x}_1} \phi_k - \frac{\bar{d}_1 T_s}{\pi L_m C_s \bar{x}_1^2} (\theta \alpha_i) \\ \frac{\bar{d}_1 T_s}{C_p} \left( \frac{V_m^2}{2L\bar{x}_1} - \frac{2V_m}{\pi L_m} - \frac{\bar{x}_2}{L_m} - \left( \frac{1}{L_m} + \frac{V_m^2}{2L\bar{x}_2^2} \right) \beta_i \right) \\ 0 \end{bmatrix}, \end{aligned}$$

where, in matrix  $B_i$ ,  $\phi_k = \phi_1$  for  $i = 1, 2$ ;  $\phi_k = \phi_2$  for  $i = 3, 4$ ;  $\alpha_i = \alpha$  for  $i = 1, 3$ ;  $\alpha_i = -\alpha$  for  $i = 2, 4$ ;  $\beta_i = \beta$  for  $i = 1, 2$ ; and  $\beta_i = -\beta$  for  $i = 3, 4$ . The grades of the membership functions of  $\tilde{x}(t)$  in the fuzzy sets  $F_{ji}$  ( $j = 1, 2$ ) are defined as:

$$M_{F_{11}}(\tilde{x}_1) = M_{F_{12}}(\tilde{x}_1) = \frac{1}{2} \left( 1 + \frac{\tilde{x}_1}{\alpha} \right);$$

$$M_{F_{13}}(\tilde{x}_1) = M_{F_{14}}(\tilde{x}_1) = \frac{1}{2} \left( 1 - \frac{\tilde{x}_1}{\alpha} \right);$$

$$M_{F_{21}}(\tilde{x}_2) = M_{F_{23}}(\tilde{x}_2) = \frac{1}{2} \left( 1 + \frac{\tilde{x}_2}{\beta} \right);$$

$$M_{F_{22}}(\tilde{x}_2) = M_{F_{24}}(\tilde{x}_2) = \frac{1}{2} \left( 1 - \frac{\tilde{x}_2}{\beta} \right).$$

Consequently, the fuzzy plant model for the error signal  $\tilde{x}(t)$  is inferred as follows:

$$\dot{\tilde{x}}(t) = \sum_{i=1}^4 \mu_i(\tilde{x}(t)) (A_i \tilde{x}(t) + B_i \tilde{d}_1(t)), \quad (8)$$

where  $\mu_i(\tilde{x}(t))$  is the normalized weighting functions dependent on  $\tilde{x}_1(t)$  and  $\tilde{x}_2(t)$ . Note that  $\sum_{i=1}^4 \mu_i(\tilde{x}(t)) = 1$  for all  $t$ . Here,  $\mu_i(\tilde{x}(t)) \geq 0$  can be defined as follows:

$$\begin{aligned} \mu_1(\tilde{x}) &= M_{F_{11}}(\tilde{x}_1) M_{F_{21}}(\tilde{x}_2); & \mu_2(\tilde{x}) &= M_{F_{12}}(\tilde{x}_1) M_{F_{22}}(\tilde{x}_2); \\ \mu_3(\tilde{x}) &= M_{F_{13}}(\tilde{x}_1) M_{F_{23}}(\tilde{x}_2); & \mu_4(\tilde{x}) &= M_{F_{14}}(\tilde{x}_1) M_{F_{24}}(\tilde{x}_2). \end{aligned}$$

To design  $\tilde{d}_1(t)$ , the concept of the parallel distributed compensation (PDC) is applied. The  $i$ th rule of the control input is described as follows:

**Control Rule  $i$ :**

IF  $\tilde{x}_1(t)$  is  $F_{1i}$  and  $\tilde{x}_2(t)$  is  $F_{2i}$  THEN  
 $\tilde{d}_1(t) = -K_i \tilde{x}(t), i = 1, 2, 3, 4.$

The integral T-S fuzzy controller in the consequent part is inferred as

$$\tilde{d}_1(t) = -\sum_{i=1}^4 \mu_i(\tilde{x}) K_i \tilde{x}(t). \quad (9)$$

By substituting (9) into (8), the closed-loop system can be represented as follows:

$$\begin{aligned} \dot{\tilde{x}}(t) &= \sum_{i=1}^4 \sum_{j=1}^4 \mu_i \mu_j (A_i - B_i K_j) \tilde{x}(t) \\ &= \sum_{i=1}^4 \sum_{j=1}^4 \mu_i \mu_j G_{ij} \tilde{x}(t). \end{aligned} \quad (10)$$

In sequence, the controller gains of the system will be derived from Lyapunov theorem.

**4. Controller Gains and Stability Analysis**

The determination of feedback gains  $K_i$  and the proof of system stability are simultaneously addressed. Choose the Lyapunov function  $V(\tilde{x}(t)) = \tilde{x}^T(t) P \tilde{x}(t) > 0$ , where  $P$  is a symmetric positive definite matrix. Taking time derivative of  $V(\tilde{x})$  along with (10), it yields

$$\dot{V}(\tilde{x}(t)) = \sum_{i=1}^4 \sum_{j=1}^4 \mu_i \mu_j \tilde{x}^T(t) (G_{ij}^T P + P G_{ij}) \tilde{x}(t).$$

Here, if we want the system (10) to be stable, it is necessary that  $P$  satisfies  $G_{ij}^T P + P G_{ij} < 0$  or a slightly stronger condition:

$$G_{ij}^T P + P G_{ij} + D P D < 0, \quad (11)$$

where the decay rate  $D$  is a diagonal positive definite matrix. After pre-multiplying and post-multiplying  $X = P^{-1}$  on (11), we can obtain

$$(A - B K_i) X + X (A^T - K_i^T B^T) + (D X)^T X^{-1} D X < 0. \quad (12)$$

Let  $M_i = K_i X$  and apply Schur's complement on (12), we can equivalently represent (11) as the following LMIs:

$$\begin{bmatrix} A_i X + X A_i^T - B_i M_j - M_j^T B_i^T & D X^T \\ D X & X \end{bmatrix} < 0. \quad (13)$$

Therefore, if there exists a common symmetric positive definite matrix  $X = P^{-1}$  such that (13) is feasible, then (8) can be exponentially stabilized via the PDC fuzzy controller (9) with  $K_i = M_i X^{-1}$ . Here,  $K_i$  is determined after  $M_i$  is obtained by solving (13) via Matlab's LMI toolbox.

According to the stability analysis, the trajectories of (10) can be regulated to the constant states (equilibrium points),  $\bar{x}$ , if (13) is feasible. That is, the output voltage can reach the prescribed value,  $V_{ref}$ , with an exponential decay rate. In addition, the decay rate of each state can be tuned by the matrix  $D$ 's related entry independently.

**5. Accomplishment of Integral T-S Fuzzy Control**

According to (6) and (9), the control input of the system (3) can be taken as follows:

$$\begin{aligned} d_1(t) &= \tilde{d}_1(t) + \bar{d}_1 \\ &= -\sum_{i=1}^4 \mu_i(\tilde{x}) \left( \begin{bmatrix} K_{i1} & K_{i2} \end{bmatrix} \begin{bmatrix} x_1 - \bar{x}_1 \\ x_2 - \bar{x}_2 \end{bmatrix} + K_{i3} (x_e - \bar{x}_e) \right) + \bar{d}_1. \end{aligned}$$

Here, the controller gains ( $K_{i1}, K_{i2}, K_{i3}$ ) can be obtained, once there exists an  $X > 0$  from (13). When the proposed controller is applied to the AHPFC converter, we notice that the variations of  $\mu_i(\tilde{x}_1)$  are often kept within a small region after the transient responses. Therefore, it is natural to let

$$\bar{x}_e = \left( \sum_{i=1}^4 \mu_i(\tilde{x}) K_{i3} \right)^{-1} \left( \bar{d}_1 - \sum_{i=1}^4 \mu_i(\tilde{x}) \begin{bmatrix} K_{i1} & K_{i2} \end{bmatrix} \begin{bmatrix} \bar{x}_1 \\ \bar{x}_2 \end{bmatrix} \right),$$

**Table 1. Parameters of the AHPFC converter.**

Parameters	Value and Unit
Peak voltage, $V_m$	156 V
Storage inductance, $L$	167.7 $\mu$ H
Exciting inductance, $L_m$	990 $\mu$ H
Storage capacitance, $C_p$	470 $\mu$ F
Output capacitance, $C_s$	10000 $\mu$ F
Full load resistance, $R_{full}$	12 $\Omega$
Light load resistance, $R_{light}$	18 $\Omega$
Switching period, $T_s$	10 $\mu$ sec
Haversine period, $T_L$	$\frac{1}{120}$ $\mu$ sec
Turns ratio of transformer, $n$	12 turn

and to regard it as the equilibrium point of  $x_e$ . The flexibility of designing  $\bar{x}_e$  is related to the robustness of the integral-type control. Consequently, the control input can be represented as

$$d_1(t) = -\sum_{i=1}^4 \mu_i(\tilde{x}) K_i x(t), \quad (14)$$

where  $K_i = [K_{i1} \ K_{i2} \ K_{i3}]$ , and  $x(t) = [x_1(t) \ x_2(t) \ x_3(t)]^T$ . Here, we notice that the controller (14) is still a nonlinear form, and we need a mass of electronic components to realize it. Fortunately, it can be simplified by the obtained controller gains from the following numerical analysis.

**IV. SOLVED GAINS AND NUMERICAL SIMULATIONS**

The proposed integral T-S fuzzy regulation is verified by the numerical simulations in this section successfully. Once the feedback controller gains are obtained, we take them into the simulations.

The associated parameter of the AHPFC converter is listed in Table 1 with the specification of the storage components. According to Table 1 and (6), the DC operating points of the states and the control input can be obtained as  $\bar{x}_1 = \bar{v}_{C_s} = 12$  V,  $\bar{x}_2 = \bar{v}_{C_p} = 222.9208$  V, and  $\bar{d}_1 = 0.2116$ . Then, we appropriately choose  $\alpha = \beta = 1$ . Based on LMIs (13) with the decay rate  $D = \text{diag}\{20.93, 1.18, 9.09\}$ , the controller gains are obtained below:

$$\begin{aligned} K_{11} = K_{21} = K_{31} = K_{41} &= 0.451896 \equiv K_{01}, \\ K_{12} = K_{22} = K_{32} = K_{42} &= 0.000647 \equiv K_{02}, \\ K_{13} = K_{23} = K_{33} = K_{43} &= -40.2411 \equiv K_{03}, \end{aligned} \quad (15)$$

where the feedback gains for every fuzzy control rule are identical. Owing to the similarities of the variables, the control law

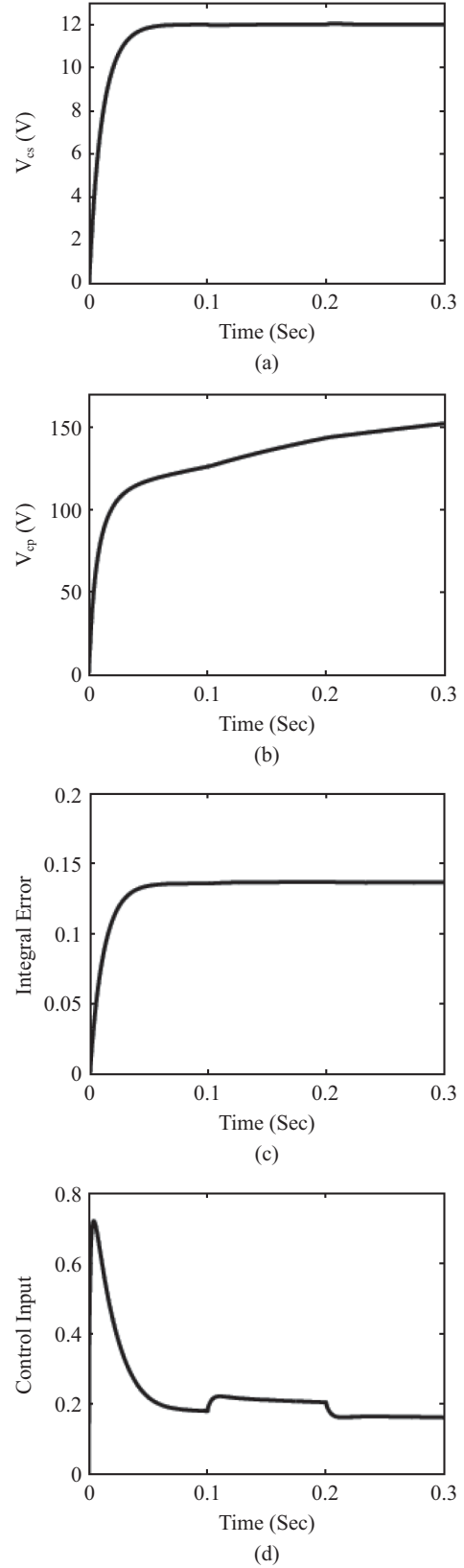


**Fig. 3. (a) Output voltage  $v_{c_s}$ , (b) capacitor voltage  $v_{c_p}$ , (c) integral error state  $x_e$ , and (d) control input of the converter, when  $R$  is changed from: 18  $\Omega$   $\rightarrow$  12  $\Omega$   $\rightarrow$  18  $\Omega$ .**

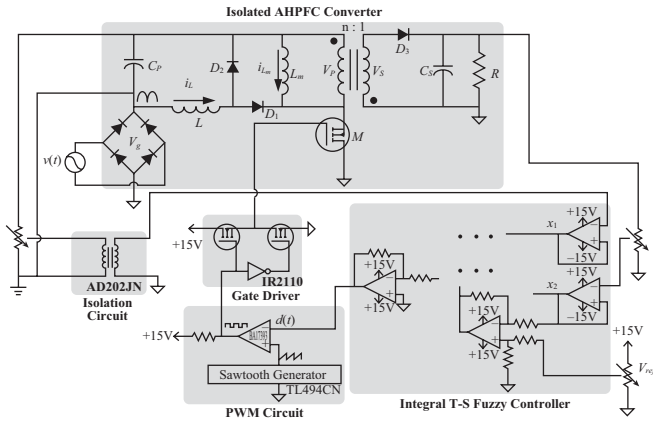


Fig. 4. Closed-loop structure of the AHPFC converter.

(14) is further reduced as  $d_1(t) \approx -K_{01}x_1 - K_{02}x_2 - K_{03}x_3$ , which is indeed a simple linear controller.

To verify the performance of the AHPFC converter with the simple integral T-S fuzzy controller, the variations of the load resistance are simulated by Matlab. The simulation results with the initial condition  $x(0) = (0, 0, 0)$  are shown in Fig. 3. It includes the controlled-plant states,  $x_1$  and  $x_2$ , the integral error state  $x_e$ , and the control input responses of the converter, when  $R$  is changed from  $18 \Omega$  to  $12 \Omega$  at  $0.1$  s, then from  $12 \Omega$  to  $18 \Omega$  at  $0.2$  s. Notice that the output voltage  $v_{Cs}$  is regulated to  $12$  V without any overshoot; the bulk capacitor voltage  $v_{Cp}$  does not reach a steady state at  $t = 0.3$  s; the integral error is very small in comparison with other states; and the control input varies within the reasonable range.

### V. CLOSED-LOOP CIRCUITS AND EXPERIMENT RESULTS

In this section, we realize the closed-loop circuits with the simplified integral T-S fuzzy controller and show the experimental results.

According to (14) with LMI-based gains (15), we can easily implement the simple controller by using analog circuits that only contain the operational amplifiers, variable resistors, resistors and capacitor. Notice that the circuits of the membership functions and the nonlinear control parts have been retrenched. The closed-loop structure of the AHPFC converter is depicted in Fig. 4. The hardware circuits contain five parts: (i) an AHPFC converter (controlled plant); (ii) a simplified integral T-S fuzzy controller; (iii) a PWM circuit; (iv) a MOSFET gate driver; and (v) an isolation circuit (AD202JN). Here, the state feedback signal  $v_{Cs}$  is measured by AD202JN and the switching driving-signal feeds to the power MOSFET via IR2110.

Sequentially, we test and show the performance of the controller via the hardware experiments. To make a comparison, all system parameters and controller gains in the experiments are

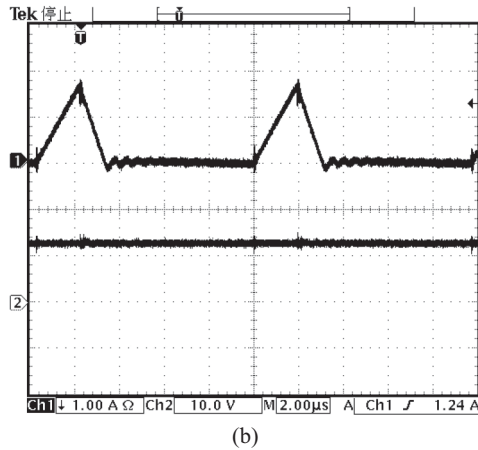
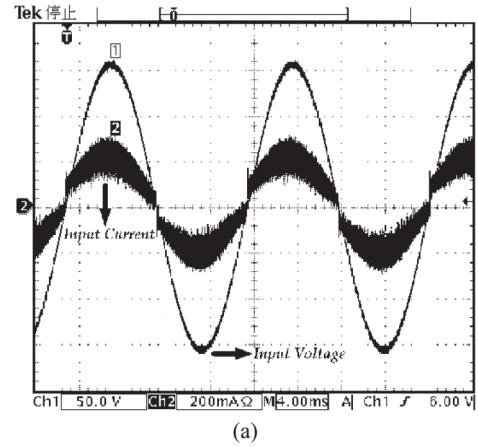
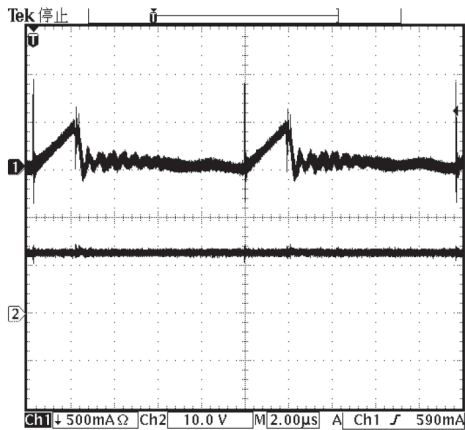


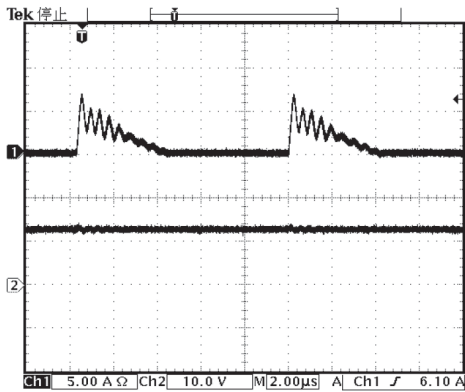
Fig. 5. (a) Input line voltage and current of the AHPFC converter. (b) The upper line is inductor current  $i_L$  and the lower line is output voltage response in DC mode.

set as the software simulations. The experimental results are shown in Figs. 5~7. In Fig 5(a), the AHPFC converter forces the input line current to follow the sinusoidal voltage. It has achieved the well power factor correction. To identify the accurate design for the inductors and transformer. In Fig. 5(b) and Fig. 6, the upper lines show that the inductor current  $i_L$  and the exciting current  $i_{Lm}$  are operated in DCM, respectively; the lower lines display that the output voltage responses are regulated to remain constant at  $12$  V in DC mode. Here, the upper lines of Figs. 6(a) and (b) are the primary current and secondary current of the transformer for  $R = 12 \Omega$ , respectively. It is indicated that the transformer is operated in correct resets with DCM conditions. Figs. 7(a) and (b) show the output voltage responses in AC mode, when  $R$  is changed from  $18 \Omega$  to  $12 \Omega$  at  $0.1$  s, then back to  $18 \Omega$  at  $0.2$  s; respectively. Here, we notice that the transient deviations are below  $0.24$  V (2% of  $12$  V) in Fig. 7. Compared with the PI controller in [14], the transient deviations are  $0.8$  V~ $1.2$  V (2%~3% of  $40$  V) and the steady state with a little high amplitude. Apparently, the performance of the proposed integral T-S fuzzy method is better than the PI controller.





(a)



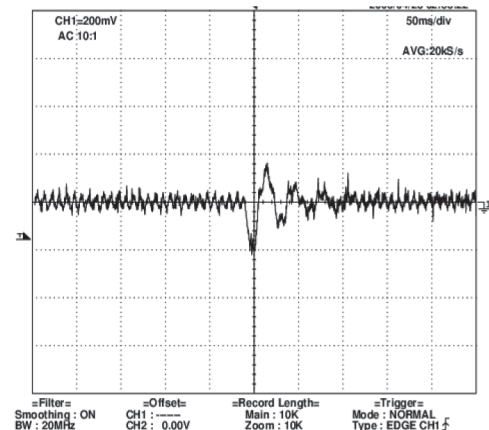
(b)

Fig. 6. The upper lines are the (a) primary current, and (b) secondary current of the transformer for  $R = 12 \Omega$ . The lower lines are output voltage responses in DC mode.

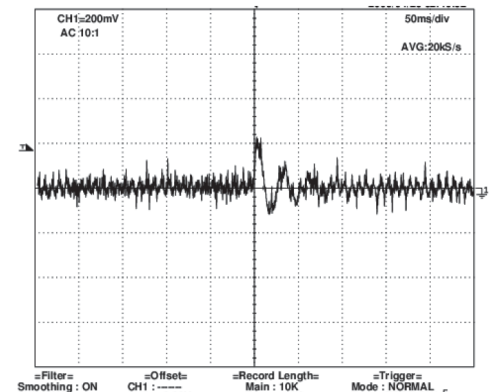
As well as the simulation results, the experimental oscillograms exhibit the perfect robustness for the variations of the load resistance. Here, the output voltage responses are always at 12 V, which provide satisfactory performances such as short setting time, low overshoot, zero steady state error and fast transient responses.

### VI. CONCLUSIONS

In this paper, the simple integral T-S fuzzy controller has achieved the power factor correction and the output voltage regulation for the AHPFC converter. The proposed control strategy can exactly model the converter with highly nonlinear dynamics. According to the feedback gains, only basic elements are necessary to realize the LMI-based fuzzy controller. Moreover, the nice input-current shapes and the small transient deviations have been verified satisfactorily in the numerical simulations and experimental results. Compared to classical linear control, the proposed scheme can cope with the nonlinear properties via a nonlinear analysis. Besides, the stability of the traditional fuzzy method has been improved by applying Lyapunov theory.



(a)



(b)

Fig. 7. Output voltage responses in AC mode, when  $R$  is changed from: (a)  $18 \Omega \rightarrow 12 \Omega$ ; (b)  $12 \Omega \rightarrow 18 \Omega$ .

### REFERENCES

1. Cao, Y.-Y. and Lin, Z., "Robust stability analysis and fuzzy-scheduling control for nonlinear systems subject to actuator saturation," *IEEE Transactions on Fuzzy Systems*, Vol. 11, No. 1, pp. 57-67 (2003).
2. Chang, W.-J., Chen, M.-W., and Ku, C.-C., "Passive fuzzy controller design for discrete ship steering systems via Takagi-Sugeno fuzzy model with multiplicative noise," *Journal of Marine Science and Technology*, Vol. 21, No. 2, pp. 159-165 (2013).
3. Chang, W.-J., Ku, C.-C., and Huang, C.-H., "Fuzzy control for input constrained passive affine Takagi-Sugeno fuzzy models: An application to truck-trailer system," *Journal of Marine Science and Technology*, Vol. 19, No. 5, pp. 470-482 (2011).
4. Chen, B.-S., Tseng, C.-S., and Uang, H.-J., "Mixed output feedback control design for nonlinear dynamic systems: An LMI approach," *IEEE Transactions on Fuzzy Systems*, Vol. 8, No. 3, pp. 249-265 (2000).
5. Chen, P.-C., Chen, C.-W., Chiang, W.-L., and Yeh, K., "A novel stability condition and its application to GA-based fuzzy control for nonlinear systems with uncertainty," *Journal of Marine Science and Technology*, Vol. 17, No. 4, pp. 293-299 (2009).
6. Cheng, K.-H., Hsu, C.-F., Lin, C.-M., Lee, T.-T., and Li, C., "Fuzzy-neural sliding-mode control for DC-DC converters using asymmetric gaussian membership functions," *IEEE Transactions on Industrial Electronics*, Vol. 54, No. 3, pp. 1528-1536 (2007).
7. He, D. and Nelms, R. M., "Fuzzy logic average current-mode control for DC-DC converters using an inexpensive 8-bit microcontroller," *IEEE Transactions on Industrial Applications*, Vol. 41, No. 6, pp. 1531-1538

- (2005).
8. Kirawanich, P. and O'Connell, R. M., "Fuzzy logic control of an active power line conditioner," *IEEE Transactions on Power Electronics*, Vol. 19, No. 6, pp. 1574-1585 (2004).
  9. Ku, C.-C., Huang, P.-H., and Chang, W.-J., "Passive fuzzy controller design for perturbed nonlinear drum-boiler system with multiplicative noise," *Journal of Marine Science and Technology*, Vol. 18, No. 2, pp. 211-220 (2010).
  10. Kugi, A. and Schlacher, K., "Nonlinear  $H_\infty$  controller design for a DC-to-DC power converter," *IEEE Transactions on Control System Technology*, Vol. 7, No. 2, pp. 230-237 (1999).
  11. Lian, K.-Y., Liou, J.-J., and Huang, C.-Y., "LMI-based integral fuzzy control of DC-DC converters," *IEEE Transactions on Fuzzy Systems*, Vol. 14, No. 1, pp. 71-80 (2006).
  12. Lian, K.-Y., Chiang, C.-H., and Tu, H.-W., "LMI-based sensorless control of permanent-magnet synchronous motors," *IEEE Transactions on Industrial Electronics*, Vol. 54, No. 5, pp. 2769-2778 (2007).
  13. Lian, K.-Y., Tu, H.-W., and Hong, C.-W., "Current sensorless regulation for converters via integral fuzzy control," *IEICE Transactions on Electronics*, Vol. E90-C, No. 2, pp. 507-514 (2007).
  14. Lin, J.-L., Chang, M.-Z., and Yang, S.-P., "Synthesis and analysis for a novel single-stage isolated high power factor correction converter," *IEEE Transactions on Circuits System I, Regular Papers*, Vol. 52, No. 9, pp. 1928-1939 (2005).
  15. Lu, D. D.-C., Lu, H. H.-C., and Pjevalica, V., "A single-stage AC/DC converter with high power factor, regulated bus voltage, and output voltage," *IEEE Transactions on Power Electronics*, Vol. 23, No. 1, pp. 218-228 (2008).
  16. Luo, S., Qiu, W., Wu, W., and Batarseh, I., "Flyboost power factor correction cell and a new family of single-stage AC/DC converters," *IEEE Transactions on Power Electronics*, Vol. 20, No. 1, pp. 25-34 (2005).
  17. Perez, M., Ortega, R., and Espinoza, J. R., "Passivity-based PI control of switched power converters," *IEEE Transactions on Control System Technology*, Vol. 12, No. 6, pp. 881-890 (2004).
  18. Perry, A. G., Feng, G., Liu, Y.-F., and Sen, P. C., "A design method for PI-like fuzzy logic controllers for DC-DC converter," *IEEE Transactions on Industrial Electronics*, Vol. 54, No. 5, pp. 2688-2696 (2007).
  19. Rubaai, A., Ofoli, A. R., Burge, L., and Garuba, M., "Hardware implementation of an adaptive network-based fuzzy controller for DC-DC converters," *IEEE Transactions on Industrial Applications*, Vol. 41, No. 6, pp. 1557-1565 (2005).
  20. Shen, M. and Qian, Z., "A novel high-efficiency single-stage PFC converter with reduced voltage stress," *IEEE Transactions on Industrial Applications*, Vol. 38, No. 2, pp. 507-513 (2002).
  21. Takagi, T. and Sugeno, M., "Fuzzy identification of systems and its applications to modeling and control," *IEEE Transactions on Systems, Man, Cybernetics*, Vol. SMC-15, No. 1, pp. 116-132 (1985).
  22. Tan, S.-C., Lai, Y. M., Tse, C. K., and Cheung, M. K. H., "Adaptive feedforward and feedback control schemes for sliding mode controlled power converters," *IEEE Transactions on Power Electronics*, Vol. 21, No. 1, pp. 182-192 (2006).
  23. Tanaka, K., Ikeda, T., and Wang, H. O., "Fuzzy regulators and fuzzy observer: Relaxed stability conditions and LMI-based designs," *IEEE Transactions on Fuzzy Systems*, Vol. 6, No. 2, pp. 250-265 (1998).
  24. Tuan, H. D., Apkarian, P., Narikiyo, T., and Yamamoto, Y., "Parameterized linear matrix inequality techniques in fuzzy control systems design," *IEEE Transactions on Fuzzy Systems*, Vol. 9, No. 2, pp. 324-332 (2001).
  25. Viswanathan, K., Oruganti, R., and Srinivasan, D., "Nonlinear function controller: A simple alternative to fuzzy logic controller for a power electronic converter," *IEEE Transactions on Industrial Electronics*, Vol. 52, No. 5, pp. 1439-1448 (2005).
  26. Wang, S.-R., Qiao, Z.-Z., and Tung, P.-C., "Application of the force control on the working path tracking," *Journal of Marine Science and Technology*, Vol. 10, No. 2, pp. 98-103 (2002).
  27. Wu, T.-F. and Chen, Y.-K., "Analysis and design of an isolated single-stage converter achieving power-factor correction and fast regulation," *IEEE Transactions on Industrial Electronics*, Vol. 46, No. 4, pp. 759-767 (1999).
  28. Zhao, Q., Xu, M., Lee, F. C., and Qian, J., "Single-switch parallel power factor correction AC-DC converters with inherent load current feedback," *IEEE Transactions on Power Electronics*, Vol. 19, No. 4, pp. 928-936 (2004).